Time-Dependent Density Functional Theory Investigation of the Electronic Spectra of Hexanuclear Chalcohalide Rhenium(III) Clusters

ARTICLE *in* THE JOURNAL OF PHYSICAL CHEMISTRY A · JANUARY 2011

Impact Factor: 2.69 · DOI: 10.1021/jp110100w · Source: PubMed

2 AUTHORS:

Jorge S. Gancheff
University of the Republic, Uruguay
45 PUBLICATIONS **332** CITATIONS
SEE PROFILE

Pablo A. Denis
University of the Republic, Uruguay
104 PUBLICATIONS **1,526** CITATIONS
SEE PROFILE

Time-Dependent Density Functional Theory Investigation of the Electronic Spectra of Hexanuclear Chalcohalide Rhenium(III) Clusters

Jorge S. Ganchef[*,†] and Pablo A. Denis[‡]

Cátedra de Química Inorgánica, Departamento "Estrella Campos", Facultad de Química, Universidad de la República, CC 1157, 11800, Montevideo, Uruguay, and Computational Nanotechnology, DETEMA, Facultad de Química, Universidad de la República, Montevideo, Uruguay

Received: October 21, 2010; Revised Manuscript Received: November 29, 2010

The UV−vis spectra of the hexanuclear chalcohalide rhenium(III) clusters of formula $[Re_6S_8X_6]^{4-}$ ($X^- = Cl^-$, Br^-, I^-) were investigated at the time-dependent density functional theory (TD-DFT) level employing B3LYP, PBE1PBE, and the double-hybrid B2PLYP functional in combination with the LANL2DZ basis set. We were able to reproduce the red shift experimentally observed when the halide changes from chloride to iodide. However, some discrepancies between experimental results and theory were found. First, we did not observe a remarkable dependence of the experimental ill-resolved bands on the solvent. Indeed, similar spectra were obtained taken CH_2Cl_2 or CH_3CN as solvents into account. Second, all calculations explained the origin of the band peaked at the low-energy region in contraposition with the one experimentally assumed by R. Long et al. (*J. Am. Chem. Soc.* **1996**, *118*, 4603), and theoretically made available by Arratia-Pérez et al. (*J. Chem. Phys.* **1999**, *110*, 2529). These authors have proposed a ligand-to-cluster charge transfer (LCCT) for all title complexes. Our findings undoubtedly allow such origin to be discarded. While the HGGA functionals lead to a cluster-to-halide ligand charge transfer (CLCT), an intracluster charge transfer (ICCT) has been considered by employing B2PLYP. This contribution showed B2PLYP in the presence of the solvent to be the best performer in studying the UV−vis spectra of large complexes of rhenium(III) containing the Re−S bond. We strongly recommended the use of the double-hybrid B2PLYP in studying UV−vis spectrum of rhenium complexes of size making the computational cost affordable. We expect that our work stimulates new experimental and theoretical investigations of the title complexes to confirm our assignment.

1. Introduction

Transition-metal clusters represent unequaled chemical compounds. Their well-defined molecular structures and their potential useful properties inherent to the metal−metal bonding make the cluster chemistry an area of utmost importance. In the rhenium-cluster chemistry, the octahedral Re_6 core plays a very important role as a molecular building block. The study of this chemistry has been extensively covered in recent years, paying particular attention at cluster containing chalcogens or halides.[1−15] Interest on such compounds is derived, for instance, from their luminescence properties associated with long emission lifetimes.[2−11] In this regard, a detailed knowledge of the electronic−structure properties is essential to provide insight into the molecular orbital constitution and to assist the experimental investigations to thoroughly understand the emissive properties and their dependence with structural changes. Theoretical studies of hexanuclear rhenium clusters can be found in the literature. In the framework of the density functional theory (DFT) in particular, the contributions of Kozlova et al.,[1] Deluzet et al.,[4] and Gray and co-workers[2,3,8] are some representatives examples regarding DFT studies of hexanuclear rhenium-clusters of formula $[Re_6S_8(CN)_6]^{4-}$,[4] $[Re_6S_8X_6]^{4-}$ ($X^- = Cl^-$, Br^-, I^-).[2,3,8] Their emissive properties were studied by the aforementioned contributions of Gray et al.[2,3,8] and the X_α calculations performed by Arratia-Pérez et al.[10] Even though a comparative study of the performance of several DFT methods to study structures of the rhenium(III) clusters $[Re_6S_8X_6]^{4-}$ ($X^- = Cl^-$, Br^-, I^-) has recently been reported,[16] there is no such a contribution to study their UV−vis spectra so far, which were experimentally studied by Gray et al.,[3] Guilbaud et al.,[9] and Long et al.[15] The origin of the ill-resolved absorption band at the visible region for all chalcohalide clusters was decided to be ligand-to-metal charge transfer (LMCT). The argument taken into account by the authors was based on the red shift observed by changing the halide ligand from Cl^- to I^-. This observation however does not allow other halide ligand-dependent charge transfer assignments to be discarded, excitation-like also leading to the red shift experimentally observed.

Herein we present comparative time-dependent DFT (TD-DFT) investigations of the rhenium(III) complexes $[Re_6S_8X_6]^{4-}$ ($X^- = Cl^-$, Br^-, I^-) by employing the standard LANL2DZ basis set[17] in combination with the hybrid-generalized-gradient-approximation functionals (HGGA) B3LYP and PBE1PBE. TD-B3LYP/LANL2DZ and TD-PBE1PBE/LANL2DZ have proved to be good performers in simulating electronic UV−vis spectra of rhenium complexes with Re−S bonds[18,19] with a very low computational cost. The double-hybrid density functional (DHDF) B2PLYP[20] was also included in this work, which has not yet been employed in studying UV−vis spectra of rhenium complexes as far as we know. The reliability of TD-B2PLYP to study UV−vis and electronic circular-dichroism (CD) spectra of small and large systems has recently made available by Grimme et al.[20−22] In calculating singlet−singlet transition like the ones investigated here, TD-B2PLYP outperforms TD-

* Author to whom correspondence should be addressed, jorge@fq.edu.uy.
† Cátedra de Química Inorgánica, Departamento "Estrella Campos", Facultad de Química.
‡ Computational Nanotechnology, DETEMA, Facultad de Química.

10.1021/jp110100w
Published on Web 12/15/2010

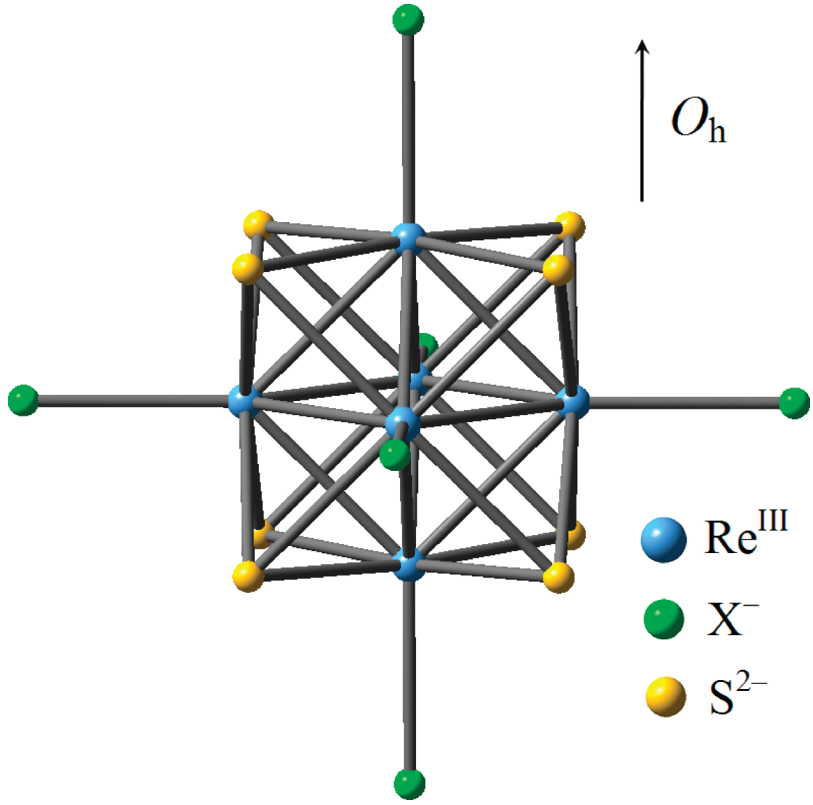

Figure 1. Geometry of the clusters of rhenium(III) $[Re_6S_8X_6]^{4-}$ ($X^- = Cl^-$, Br^-, I^-) optimized employing B3LYP, PBE1PBE, and the DHDF B2PLYP functional.

B3LYP by using a medium-size basis set.[22] This behavior was expected because the B2PLYP method belongs to the fifth-rung in Perdew's scheme of Jacob's ladder, these DHDFs offering a high chemical accuracy for broad applications to be reachable.[23−26] However, the larger computational cost of B2PLYP as compared with B3LYP is not always justified. An example is given by the calculation of anharmonic vibrational frequencies as showed by Biczysko et al.[27] The extra computational cost of B2PLYP is due to the substitution to some extent of a correlation functional by mixing in a nonlocal perturbative correlation.

The inclusion of B2PLYP in this work was decided, intending to expand its range of application by testing its reliability to study the absorptive features of rhenium complexes. All results presented in this work allow us to discard a halide ligand-to-cluster charge transfer (LCCT) as origin of the band at the low-energy part of the spectrum. The assignments proposed by us differ from the experimental assignment[3,9,15] and from the X_α results reported by Arratia-Pérez et al.[10] It is worth mentioning that the assignment CLCT observed in this work by employing HGGA-based methods resulted in concordance with the character experimentally proposed for a similar band of analogous rhenium(III) cyanide-bridged cluster reported by Shores and coworkers.[28] Finally, our work provides new evidence confirming the superior performance of the fifth-rung density functional as compared with the traditional HGGA like the ones included in this work.

2. Computational Details

All calculations have been carried out at the time-dependent density functional theory (TD-DFT) level of theory. To study UV−vis spectra of a hexanuclear cluster of Re(III), we have employed the B3LYP and PBE1PBE methods[29−34] in conjunction with the standard LANL2DZ basis set. The DHDF B2PLYP[20] functional was also employed taken its outperformance with respect to B3LYP showed in studying singlet−singlet excitations like the one considered here into account.[22] To the best of our knowledge, no UV−vis spectra of rhenium complexes were studied by means of TD-B2PLYP so far (the label "TD" will be omitted hereafter). Besides the study of the electronic features of the complexes included in this work, it is also our aim to test the reliability of B2PLYP in simulating UV−vis spectra of rhenium complexes and, in doing so, to expand the range of application of this functional. LANL2DZ takes scalar relativistic effects into account, especially important when systems with transition metal atoms are studied.[35]

To simulate the absorption spectra, we have followed this procedure:

(1) the geometries of the clusters $[Re_6S_8X_6]^{4-}$ ($X^- = Cl^-$, Br^-, I^-) (Figure 1) were optimized in the O_h symmetry point group, for which the closed-shell singlet ($S = 0$) state was considered.

(2) The nature of the stationary point was verified through a analytical vibrational analysis (no imaginary frequencies at the minimum).

(3) Vertical energy transitions at the equilibrium geometry within the TD-DFT approach are calculated. One hundred fifty singlet−singlet spin-allowed excitations were calculated in the gas phase and in solution. The bulk solvent effects were treated by means of the conductor-like polarizable continuum model (C-PCM),[36,37] which is a valid model to take the effects of the solvent into account as long as specific interactions between the solute and the solvent are not of significant importance. Dichloromethane (CH_2Cl_2) and acetonitrile (CH_3CN) were selected as solvents considering the experimental data.[3,9,15]

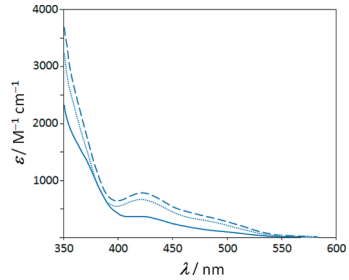

Figure 2. Absorption spectra simulated with GaussSum of $[Re_6S_8Cl_6]^{4-}$ as obtained employing B2PLYP in the gas phase (—), and in the presence of CH_2Cl_2 (---), or CH_3CN (•••).

(4) Once the results of step 3 are obtained, the absorption spectra are simulated employing the GaussSum software[38] including all calculated electronic transitions.

The discussion of results obtained with all methodologies for each cluster separately is presented first, a comparative study being presented thereafter. It is worth mentioning, that only the results in the low-energy part of the spectrum (350−600 nm) are presented and discussed taken the experimental information[3,9,15] into account.

All DFT calculations reported in this work have been conducted by means of the software package Gaussian 09, Rev. A.01.[39]

3. Results and Discussion

a. $[Re_6S_8Cl_6]^{4-}$. In the gas phase, one absorption band was detected in the simulated UV−vis spectrum employing B3LYP/LANL2DZ or PBE1PBE/LANL2DZ (Figures S1 and S2 in the Supporting Information) ("LANL2DZ" will be hereafter omitted). In both cases a blue shift with respect to the experimental evidence[3,9,15] was observed, with the last method being the most important one (−69 nm). The results in CH_2Cl_2 or CH_3CN did not markedly differ with respect to the one calculated in the gas phase (Figures S1 and S2 in the Supporting Information). This finding is in disagreement with the experimental results[3,9,15] that show some dependence of ill-resolved bands on the solvent. In the presence of the solvent one absorption band was detected, for which a hypsochromic shift of −7 nm with respect to the results in the gas phase is calculated.

When the results obtained with B2PLYP are analyzed, interesting features emerge. The simulated spectra in the gas phase and in the presence of the solvent are displayed in Figure 2. Despite experimentally ill-resolved absorption bands, it is clear that agreement with the experimental spectrum is improved as compared with the B3LYP or PBE1PBE results. Even in the gas phase, the simulation accounts for the absorption band and shoulders exhibited by the experimental spectra.[9,15]

A well-defined absorption band was calculated at 423 nm, for which a hypsochromic shift of −12 nm with respect to the experimental value was calculated.[9,15] Spectra featured by a band peaked at 421 nm were simulated by inclusion of the solvent, an observation in line with the one observed in the gas phase. The solvent induces all bands to be more intense with respect to the result in the gas phase. When the experimental values of the molar absorption coefficients (ε) are considered,[9,15] the results with B2PLYP in the presence of CH_2Cl_2 or CH_3CN represent the best simulation of the experimental spectrum.

The orbital excitations leading to the well-defined absorption band previously mentioned are summarized in Table 1. By employing all methodologies in the gas phase and in the presence of the solvent, three excitation groups are responsible for the detected band, in all of them the electron being transferred from the HOMO−1 and HOMO. With B3LYP in

TABLE 1: Selected Orbital Excitations Calculated for $[Re_6S_8Cl_6]^{4-}$ in the Gas Phase and in the Presence of the Solvent (CH_2Cl_2 or CH_3CN) Employing B3LYP, PBE1PBE, and B2PLYP in Combination with the LANL2DZ Basis Set[a]

method[b]	λ (nm)	*f*	excitations[c]	assignment[d]
B3LDZ/gas	398.0	0.0057	H−1 → L+4, H−1 → L+6, H → L+4, H → L+5	
	398.0	0.0057	H−1 → L+4, H → L+5	CLCT
	398.0	0.0057	H−1 → L+5, H → L+6	
B3LDZ/CH_2Cl_2	392.6	0.0096	H−1 → L+4, H → L+5, H−1 → L+5	
	392.6	0.0096	H−1 → L+4, H → L+5, H−1 → L+5	CLCT
	392.6	0.0096	H−1 → L+6	
B3LDZ/CH_3CN	392.0	0.0087	H−1 → L+4, H → L+5	
	392.0	0.0087	H−1 → L+4, H → L+5	CLCT
	392.0	0.0087	H−1 → L+4, H−1 → L+6, H → L+6	
PBLDZ/gas	364.7	0.0075	H−1 → L+4, H → L+4, H → L+5	
	364.7	0.0075	H−1 → L+5, H → L+4, H → L+5	CLCT
	364.7	0.0075	H−1 → L+6	
PBLDZ/CH_2Cl_2	359.8	0.0123	H−1 → L+7, H → L+7	
	359.8	0.0123	H−1 → L+8, H → L+8	CLCT
	359.8	0.0123	H−1 → L+9	
PBLDZ/CH_3CN	359.3	0.0112	H → L+7	
	359.3	0.0112	H−1 → L+8, H → L+8	CLCT
	359.3	0.0112	H−1 → L+9, H → L+9	
B2PLDZ/gas	422.7	0.0015	H → L+4, H → L+5	
	422.5	0.0015	H−1 → L+5, H → L+5, H → L+6	ICCT
	422.4	0.0015	H−1 → L+4, H−1 → L+6	
B2PLDZ/CH_2Cl_2	421.3	0.0034	H → L+4, H → L+5	
	421.2	0.0034	H−1 → L+5, H → L+4, H → L+5	ICCT
	421.0	0.0034	H−1 → L+4, H−1 → L+6	
B2PLDZ/CH_3CN	421.0	0.0030	H → L+4, H → L+5, H → L+6	
	420.9	0.0030	H−1 → L+5, H → L+4, H → L+5	ICCT
	420.7	0.0030	H−1 → L+4, H−1 → L+6	

[a] Only those excitations with contribution over 10% have been considered. [b] B3LDZ = B3LYP/LANL2DZ; PBLDZ = PBE1PBE/LANL2DZ; B2PLDZ = B2PLYP/LANL2DZ. [c] H = HOMO; L = LUMO. [d] See in text for acronyms employed in assigning origin of absorption bands.

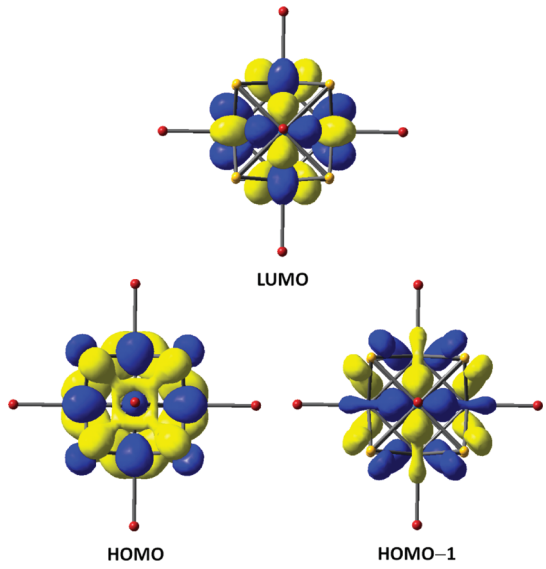

Figure 3. Contour of the HOMO, HOMO−1, and LUMO of $[Re_6S_8X_6]^{4-}$ ($X^- = Cl^-$, Br^-, I^-) as obtained by employing the B3LYP, PBE1PBE, and B2PLYP.

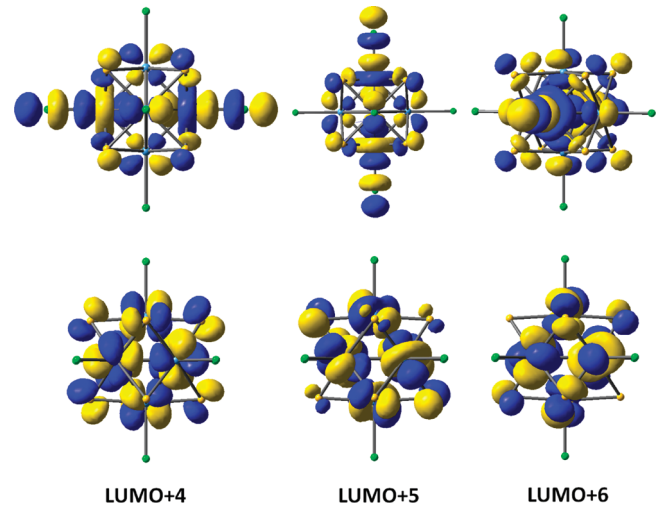

Figure 4. Contour of the LUMO+4, LUMO+5, and LUMO+6 of $[Re_6S_8Cl_6]^{4-}$ as obtained by employing B3LYP and PBE1PBE (top) and B2PLYP (bottom). They become the LUMO+7, LUMO+8, and LUMO+9, respectively, by inclusion of the solvent with PBE1PBE.

the gas phase and in the presence of the solvent, the electron transfer takes place in the orbitals LUMO+4, LUMO+5, and LUMO+6. With PBE1PBE the situation is identical. However, the order of the MOs is slightly changed by inclusion of the solvent (see Table 1). Indeed, LUMO+4, LUMO+5, and LUMO+6 in the gas phase become LUMO+7, LUMO+8, and LUMO+9 in CH_2Cl_2 or CH_3CN.

The results with B2PLYP in the gas phase and in the presence of the solvent lead the LUMO+4, LUMO+5, and LUMO+6 to be the final MOs in all cases.

Our findings show orbitals other than the LUMO involved in the excitations are in line with that reported by Deluzet et al.[4] They have proposed in the framework of the zero-order regular approximation (ZORA), that molecular orbitals other than HOMO, HOMO−1, LUMO, and LUMO+1 must be implicated in the origin of the lowest-energy absorption band analyzed in this work.

Interesting features can be observed when the contours of the aforementioned MOs are considered. The frontier orbitals HOMO and LUMO are calculated with *all methods* as mainly centered on the metal atoms (Figure 3). The HOMO—that resulted double-degenerated (e_g)—shows a high contribution from rhenium $d_{x^2-y^2}$ orbital, the LUMO being constituted exclusively of rhenium d orbitals. These observations agree with that reported by Gray et al.[3] and Deluzet et al.[4] The contours of LUMO+4, LUMO+5, and LUMO+6 obtained with the HGGA functionals are showed in Figure 4 (top). They are largely antibonding in character and centered along the rhenium−halide bond. It is worth remembering that these orbitals become the LUMO+7, LUMO+8, and LUMO+9 ones, respectively, with PBE1PBE in CH_2Cl_2 or CH_3CN.

The LUMO derivatives involved in the excitations originating with the band calculated at 421 nm with B2PLYP, namely, LUMO+4, LUMO+5, and LUMO+6, exhibit interesting characteristics (Figure 4, bottom). Unlike the one calculated with the HGGA functionals, these MOs are rather mainly cluster-centered with important contributions from rhenium d and sulfur p orbitals.

The results obtained with B3LYP and PBE1PBE allow the origin of the band calculated around 395 nm to be mainly CLCT. However, the results with B2PLYP clearly point to the assignment of the band calculated at about 420 nm to be mainly ICCT. These findings differ from the one reported,[3,10,15] in which a halide ligand-to-metal charge transfer (LCCT) has been experimentally and theoretically considered. Despite the different assignments observed by changing the methodology, all results observed for $[Re_6S_8Cl_6]^{4-}$ undoubtedly allow us to discard a LCCT as the origin of the band experimentally detected at 434 nm.

It is worth mentioning that the destination LUMO derivatives resulted in triply degenerate orbitals, for which a Jahn−Teller splitting is expected. It may proceed by vibronic coupling effect or by structural distortion of the excited state with respect to the ground state geometry. We assumed this distortion to be small enough to keep our *qualitative* description of MOs valid and, hence, the proposed assignment for the absorption band under study. The same assumption is made for complexes $[Re_6S_8Br_6]^{4-}$ and $[Re_6S_8I_6]^{4-}$.

b. $[Re_6S_8Br_6]^{4-}$. One well-defined absorption band was simulated by employing all methodologies based on HGGA functionals (Figures S3 and S4 in the Supporting Information). With B3LYP and PBE1PBE in the gas phase, a band peaked at 422 and 378 nm, respectively, were observed, −21 and −65 nm blue-shifted with respect to the experimental result.[15] In the presence of the solvent, a more pronounced hypsochromic effect was obtained. With respect to the blue shift calculated in the gas phase, the inclusion of CH_2Cl_2 led to a value of −14 nm with B3LYP and of −6 nm with PBE1PBE, the hypsochromic effect taking place in CH_3CN practically in the same extension.

When the DHDF functional is used, differences with respect to the previous results become visible, as can be seen in Figure 5. In contraposition to the one already discussed, B2PLYP in the gas phase accounts only for the presence of a shoulder and ill-resolved absorption bands. The one analyzed in this work has been detected at 425 nm, −18 nm blue-shifted with respect to the experimental value of 443 nm.[15] By considering the bulk effect of the solvent, the simulation leads to spectra in which the poor resolution of the absorption band is more evident. This observation is in line with the one observed by changing the halide ligand from Cl^- to Br^-.[15] A band at 424 nm was simulated, which resulted hypsochromically shifted in the same extension as in the gas phase. It is interesting to note that all methodologies lead to the absorption band of $[Re_6S_8Br_6]^{4-}$ being

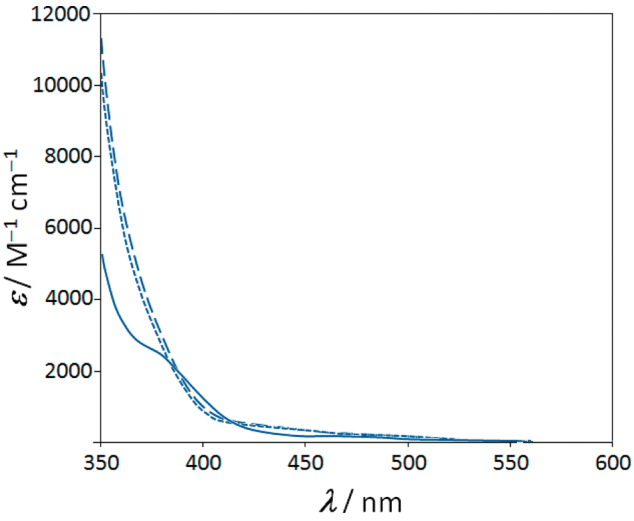

Figure 5. Absorption spectra simulated with GaussSum of $[Re_6S_8Br_6]^{4-}$ as obtained by employing B2PLYP in the gas phase (—), and in the presence of CH_2Cl_2 (- - -), or CH_3CN (• • •).

more intense with respect to the one simulated for $[Re_6S_8Cl_6]^{4-}$, an observation in agreement with the one experimentally detected by Long et al.[15]

In Table 2 the most important orbital excitations associated with the band experimentally located at 443 nm are presented. In analogy with the foregoing results of $[Re_6S_8Cl_6]^{4-}$, three excitation groups originate the detected band for the cluster containing bromide. However, excitations from MOs other than the HOMO and HOMO−1 are also observed in the gas phase by using the HGGA functionals (Table 2). Indeed, the density transfer occurs from the HOMO−7, HOMO−6, HOMO−5,

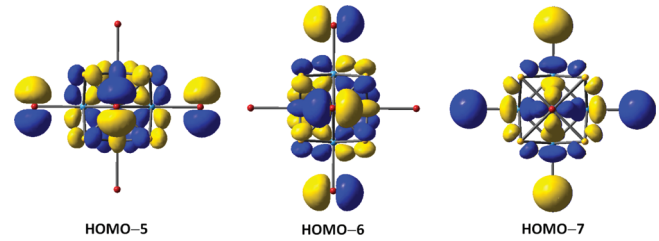

Figure 6. Contour of selected HOMO derivatives of $[Re_6S_8Br_6]^{4-}$ as obtained by employing B3LYP and PBE1PBE.

HOMO−1, and HOMO. The final MOs are the LUMO+4, LUMO+5, and LUMO+6 with some exception, which also include the LUMO. The orbitals lying beneath the HOMO−1 and HOMO already mentioned are mainly cluster-centered MOs, for which a contribution from the p orbital of the bromide can be also observed (Figure 6). The LUMO+4, LUMO+5, and LUMO+6 are calculated with similar contours as the one observed for the chloride-containing cluster (Figure 4). Since they are orbitals centered along the rhenium−halide bond, the origin of the band experimentally detected at 443 nm may be considered to be *mainly* CLCT.

The situation in the presence of the solvent is similar. With the exception of a minor contribution (16%) coming from the excitation HOMO−6 → L (B3LYP/CH_2Cl_2), the other ones take place from the HOMO−1 and HOMO to the LUMO+4, LUMO+5, and LUMO+6. Therefore, and in line with the one discussed for $[Re_6S_8Cl_6]^{4-}$, a CLCT in CH_2Cl_2 or CH_3CN may be clearly assumed.

The excitations calculated with B2PLYP for the band simulated at about 424 nm resemble the one observed for $[Re_6S_8Cl_6]^{4-}$. The presence of the solvent does no introduce

TABLE 2: Selected Orbital Excitations Calculated for $[Re_6S_8Br_6]^{4-}$ in the Gas Phase, and in the Presence of the Solvent (CH_2Cl_2 or CH_3CN) Employing B3LYP, PBE1PBE, and B2PLYP in Combination with the LANL2DZ Basis Set[a]

method[b]	λ (nm)	*f*	excitations[c]	assignment[d]
B3LDZ/gas	422.2	0.0032	H−7 → L, H−1 → L+5, H−1 → L+6, H → L+5	
	422.2	0.0032	H−6 → L, H → L+4	CLCT
	422.2	0.0032	H−5 → L, H−1 → L+6	
B3LDZ/CH_2Cl_2	407.8	0.0105	H → L+4, H → L+5	
	407.8	0.0105	H−1 → L+4, H → L+4, H → L+5	CLCT
	407.8	0.0105	H−6 → L, H−1 → L+6	
B3LDZ/CH_3CN	406.8	0.0099	H−1 → L+4, H−1 → L+6, H → L+5, H → L+6	
	406.8	0.0099	H−1 → L+6, H → L+5	CLCT
	406.8	0.0099	H−1 → L+4, H → L+4, H → L+5	
PBLDZ/gas	378.2	0.0068	H−5 → L, H−1 → L+6, H → L+6	
	378.2	0.0068	H−6 → L, H−1 → L+4, H → L+4	CLCT
	378.2	0.0068	H−7 → L, H → L+5	
PBLDZ/CH_2Cl_2	371.7	0.0142	H−1 → L+5, H → L+5	
	371.7	0.0142	H−1 → L+4, H → L+4	CLCT
	371.7	0.0142	H−1 → L+6	
PBLDZ/CH_3CN	370.8	0.0131	H−1 → L+4, H → L+4	
	370.8	0.0131	H−1 → L+5, H → L+5	CLCT
	370.8	0.0131	H → L+6	
B2PLDZ/gas	425.3	0.0007	H → L+4	
	425.2	0.0007	H−1 → L+5, H → L+5	ICCT
	425.1	0.0007	H−1 → L+6	
B2PLDZ/CH_2Cl_2	424.1	0.0022	H → L+4	
	423.9	0.0022	H−1 → L+5, H → L+5	ICCT
	423.8	0.0022	H−1 → L+6, H → L+6	
B2PLDZ/CH_3CN	423.8	0.0019	H → L+4	
	423.6	0.0019	H−1 → L+5, H → L+5	ICCT
	423.5	0.0019	H−1 → L+6, H → L+6	

[a] Only those excitations with contribution over 10% have been considered. [b] B3LDZ = B3LYP/LANL2DZ; PBLDZ = PBE1PBE/LANL2DZ; B2PLDZ = B2PLYP/LANL2DZ. [c] H = HOMO; L = LUMO. [d] See in text for acronyms employed in assigning origin of absorption bands.

TABLE 3: Selected Orbital Excitations Calculated for $[Re_6S_8I_6]^{4-}$ in the Gas Phase, And in the Presence of the Solvent (CH_2Cl_2 or CH_3CN) Employing B3LYP, PBE1PBE, and B2PLYP in Combination with the LANL2DZ Basis Set[a]

method[b]	λ (nm)	f	excitations[c]	assignment[d]
B3LDZ/gas	441.8	0.0063	H−1 → L+2, H → L+2	
	441.8	0.0063	H−1 → L+1, H → L+1	CLCT
	441.8	0.0063	H → L+3	
B3LDZ/CH_2Cl_2	422.6	0.0141	H−2 → L, H−1 → L+4, H−1 → L+5	
	422.6	0.0141	H−3 → L, H−1 → L+4, H → L+5	CLCT
	422.6	0.0141	H−4 → L, H−1 → L+6, H → L+6	
B3LDZ/CH_3CN	420.9	0.0137	H−1 → L+4, H → L+5	
	420.9	0.0137	H−1 → L+5, H → L+4, H → L+5	CLCT
	420.9	0.0137	H → L+6	
PBLDZ/gas	402.0	0.0059	H−5 → L, H → L+4	
	402.0	0.0059	H−1 → L+5, H−1 → L+6, H → L+4, H → L+5	CLCT
	402.0	0.0059	H−1 → L+5, H−1 → L+6, H → L+5	
PBLDZ/CH_2Cl_2	383.2	0.0197	H−1 → L+4, H → L+5	
	383.2	0.0197	H−1 → L+5	CLCT
	383.2	0.0197	H−1 → L+4, H → L+6	
PBLDZ/CH_3CN	381.6	0.0184	H−1 → L+4, H → L+6	
	381.6	0.0184	H−1 → L+4, H−1 → L+5, H−1 → L+6, H → L+4	CLCT
	381.6	0.0184	H → L+5, H → L+6	
B2PLDZ/gas	428.6	0.0001	H → L+4, H → L+5	
	428.5	0.0001	H−1 → L+4, H → L+4, H → L+6	ICCT
	428.5	0.0001	H−1 → L+4, H−1 → L+6	
B2PLDZ/CH_2Cl_2	427.5	0.0008	H−1 → L+5	
	427.4	0.0008	H−1 → L+4, H → L+4, H → L+5, H → L+6	ICCT
	427.3	0.0008	H−1 → L+4, H → L+6	
B2PLDZ/CH_3CN	427.3	0.0007	H−1 → L+5, H → L+4	
	427.2	0.0007	H−1 → L+4, H → L+4, H → L+5, H → L+6	ICCT
	427.1	0.0007	H−1 → L+4, H → L+6	

[a] Only those excitations with contribution over 10% have been considered. [b] B3LDZ = B3LYP/LANL2DZ; PBLDZ = PBE1PBE/LANL2DZ; B2PLDZ = B2PLYP/LANL2DZ. [c] H = HOMO; L = LUMO. [d] See in text for acronyms employed in assigning origin of absorption bands.

changes with respect to the situation in the gas phase. The charge in all excitations moves from the HOMO and HOMO−1 to the LUMO+4, LUMO+5, and LUMO+6. Their contours remain unaltered by changing the halide ligand and indeed resulted similar to the one observed for $[Re_6S_8Cl_6]^{4-}$ (Figure 4). Therefore, an ICCT can be considered for the band at about 424 nm.

c. $[Re_6S_8I_6]^{4-}$. In the gas phase and in the presence of the solvent, one absorption band was observed for this complex by employing B3LYP or PBE1PBE (Figures S5 and S6 in the Supporting Information). In the gas phase it was calculated at 442 nm with B3LYP, −65 nm blue-shifted with respect to the experimental value of 507 nm (Table 3).[15] With PBE1PBE a hypsochromic-shift of −105 nm was observed. The maximum of the absorption band moves hypsochromically when the solvent is considered. A more pronounced blue shift with respect to the results in the gas phase is calculated in the presence of CH_2Cl_2 or CH_3CN, being of −20 nm in both cases.

From the simulation by means of B2PLYP resulted spectra, in which the poor resolution of the absorption band is more pronounced taken the one observed for $[Re_6S_8Cl_6]^{4-}$ and $[Re_6S_8Br_6]^{4-}$ into account (see Figure 7). This observation agrees with the experimental evidence.[15] However, an absorption band peaked at 428 nm could be detected. This finding does not show dependence on the solvent and, indeed, practically no blue shift with respect to the gas phase was observed. Once again, the change of the halide ligand from Br^- to I^- leads the value of ε to increase, an observation in line with that reported by Long et al.[15]

For this cluster, three groups of excitations also originate the band experimentally located at 507 nm. In almost all cases the charge moves from the HOMO−1 and HOMO. However, minor contributions from excitations involving the HOMO−2, HO-

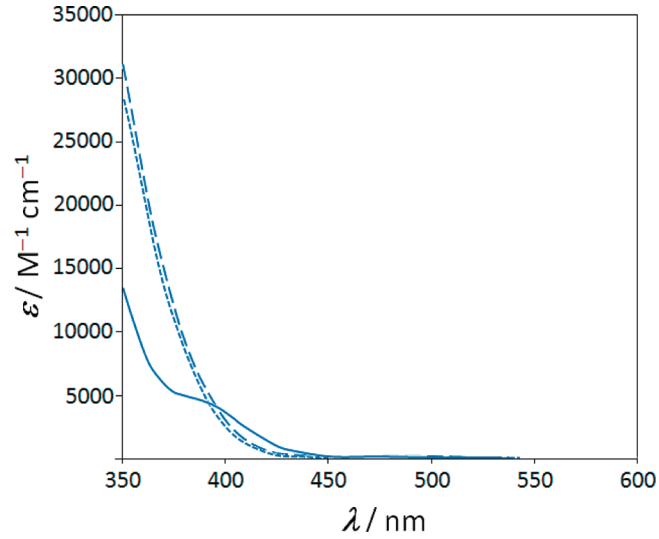

Figure 7. Absorption spectra simulated with GaussSum of $[Re_6S_8I_6]^{4-}$ as obtained employing B2PLYP in the gas phase (—) and in the presence of CH_2Cl_2 (---), or CH_3CN (•••).

MO−3, HOMO−4 (with B3LYP/CH_2Cl_2), and the HOMO−5 (with PBE1PBE/gas) have been observed (contours displayed in Figure 8). In the gas phase the final MOs are the LUMO+1, LUMO+2, and LUMO+3. In CH_2Cl_2 or CH_3CN they become the LUMO+4, LUMO+5, and LUMO+6. All of them are orbitals that are large antibonding in character and centered along the rhenium−iodide bond. These findings account for destination MOs with similar features with respect to that calculated for $[Re_6S_8Cl_6]^{4-}$ and $[Re_6S_8Br_6]^{4-}$ by employing the HGGA-based methods. These observations point to the origin of the band experimentally peaked at 507 nm by employing HGGA functionals to be *mainly* CLCT.

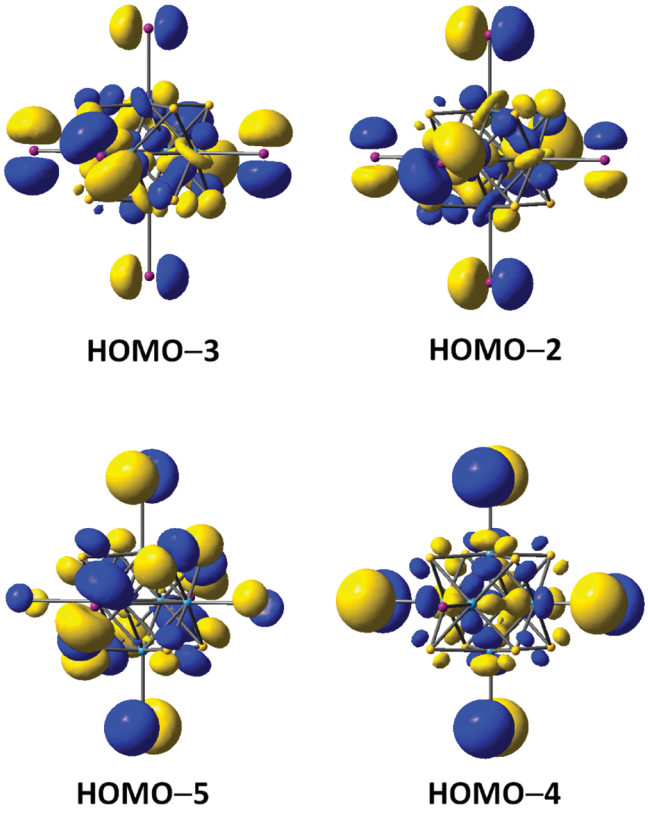

Figure 8. Contour of selected HOMO derivatives of $[Re_6S_8I_6]^{4-}$ as obtained by employing B3LYP and PBE1PBE.

The results obtained with B2PLYP did not differ with respect to the one calculated for $[Re_6S_8Cl_6]^{4-}$ and $[Re_6S_8Br_6]^{4-}$, an observation in line with a consistent behavior of this DHDF functional. The LUMO+4, LUMO+5, and LUMO+6 are the final MOs, which makes it possible to assume an ICCT as origin of the band studied in this work for $[Re_6S_8I_6]^{4-}$.

4. Comparative Studies

With the HGGA functionals in the gas phase and in the presence of the solvent (CH_2Cl_2 or CH_3CN), one well-defined absorption band was detected in the range 350−600 nm for all complexes included in this contribution. In all cases, the maximum of the absorption band is simulated hypsochromically shifted with respect to the experimental value.[3,9,15] The shift is methodology and halide ligand dependent, ranging from −21 nm (B3LYP/gas on $[Re_6S_8Br_6]^{4-}$) to −125 nm (PBE1PBE/gas on $[Re_6S_8I_6]^{4-}$) (Table 4). In this last case it deserves to be remarked that the experimental value of 507 nm has been not directly determined but through an extrapolation.[15] The presence of the solvent do not seem to introduce important changes in the position of the maximum but in its intensity. The combination of LANL2DZ with both HGGA functionals was able to reproduce the red shift observed when the halide changes.[15]

B2PLYP leads to simulated spectra accounting for all details showed by the experimental ones.[3,9,15] A hypsochromic shift was obtained in all cases. It is of up to −80 nm (PBE1PBE/gas on $[Re_6S_8I_6]^{4-}$), this case deserving the same previous comment as already made for the performance of the HGGA functionals. Similar to the foregoing results, the solvent does not play an important role in the maximum of the band but in its value of ε. B2PLYP was also able to detect a red shift by changing the halide ligand. This functional also leads to a lose of resolution of the simulated spectra in going from Cl^- to I^-, observations in agreement with the experimental evidence obtained by Long et al.[15]

TABLE 4: Summarized TD-DFT Results for $[Re_6S_8X_6]^{4-}$ ($X^- = Cl^-, Br^-, I^-$) by Employing Different DFT Methodologies

cluster	method[a]	λ (nm)[b]	blue shift (nm)[c]	assignment[d]
$[Re_6S_8Cl_6]^{4-}$	B3LDZ/gas	398.0	−36	CLCT
	B3LDZ/CH_2Cl_2	392.6	−41	CLCT
	B3LDZ/CH_3CN	392.0	−42	CLCT
	PBLDZ/gas	364.7	−69	CLCT
	PBLDZ/CH_2Cl_2	359.8	−74	CLCT
	PBLDZ/CH_3CN	359.3	−75	CLCT
	B2PLDZ/gas	422.7	−11	ICCT
	B2PLDZ/CH_2Cl_2	421.2	−12	ICCT
	B2PLDZ/CH_3CN	420.9	−12	ICCT
$[Re_6S_8Br_6]^{4-}$	B3LDZ/gas	422.2	−21	CLCT
	B3LDZ/CH_2Cl_2	407.8	−35	CLCT
	B3LDZ/CH_3CN	406.8	−36	CLCT
	PBLDZ/gas	378.2	−65	CLCT
	PBLDZ/CH_2Cl_2	371.7	−71	CLCT
	PBLDZ/CH_3CN	370.8	−72	CLCT
	B2PLDZ/gas	425.2	−18	ICCT
	B2PLDZ/CH_2Cl_2	423.9	−19	ICCT
	B2PLDZ/CH_3CN	423.6	−19	ICCT
$[Re_6S_8I_6]^{4-}$	B3LDZ/gas	441.8	−65	CLCT
	B3LDZ/CH_2Cl_2	422.6	−84	CLCT
	B3LDZ/CH_3CN	420.9	−85	CLCT
	PBLDZ/gas	402.0	−105	CLCT
	PBLDZ/CH_2Cl_2	383.2	−124	CLCT
	PBLDZ/CH_3CN	381.6	−125	CLCT
	B2PLDZ/gas	428.5	−79	ICCT
	B2PLDZ/CH_2Cl_2	427.4	−80	ICCT
	B2PLDZ/CH_3CN	427.2	−80	ICCT

[a] B3LDZ = B3LYP/LANL2DZ; PBLDZ = PBE1PBE/LANL2DZ; B2PLDZ = B2PLYP/LANL2DZ. [b] Average value for B2PLYP/LANL2DZ. [c] Blue shifts with respect to the experimental values taken from ref 15. [d] See in text for acronyms employed in assigning origin of absorption bands.

In the analysis of the origin of the absorption band studied in this work, three groups of excitations have been calculated for all complexes by employing all functionals. In general, the excitations have been calculated starting from the HOMO and the HOMO−1, orbitals with a high contribution from rhenium $d_{x^2-y^2}$ orbital. However, exceptions were obtained for $[Re_6S_8Br_6]^{4-}$ and $[Re_6S_8I_6]^{4-}$ by employing the HGGA functionals. While for the former complex excitations from the HOMO−5, HOMO−6, and HOMO−7 have been additionally obtained, excitations from the HOMO−2, HOMO−3, HOMO−4, and HOMO−5 were also observed for the last one. The final MOs in all cases resulted in large antibonding character centered along the rhenium−halide bond. B2PLYP behaves consistently and leads to identical excitations for all clusters, in which the charge is transferred from the HOMO and the HOMO−1 to LUMO derivatives mainly centered on the cluster.

When the assignment of the origin of the studied band is analyzed, differences from the behavior of the methodologies aforementioned become evident. The results HGGA-functional-based allow the origin of the band to be cluster-to-halide ligand charge transfer (CLCT). With B2PLYP an intracluster charge transfer (ICCT) may be considered in all cases. Despite the differences in ascribing the origin of the band, all results undoubtedly discard a halide ligand-to-cluster charge transfer (LCTC), an observation in contraposition to the one stated by the experimentalists[3,9,15] and by Arratia-Pérez and co-workers.[10]

5. Conclusions

Herein we present for the first time, comparative TD-DFT investigations of the UV−vis spectra of hexanuclear rhe-

nium(III) clusters of formula $[Re_6S_8X_6]^{4-}$ ($X^- = Cl^-$, Br^-, I^-) by means of combination of LANL2DZ with B3LYP, PBE1PBE, and the double-hybrid B2PLYP functional.

With the HGGA functionals, we were able to reproduce the red shift experimentally observed when the halide changes from chloride to iodide. Some discrepancies with that reported were found. We did not observe a remarkable dependence of the position of the simulated band on the solvent, and similar spectra were obtained in the presence of CH_2Cl_2 or CH_3CN.

With B2PLYP, spectra accounting for all details experimentally observed by Long et al.[15] were observed, which also led to a bathochromic displacement of the absorption band upon changing the halide ligand from Cl^- to I^-. The error in the maximum introduced by this functional in simulating the absorption band is smaller than the corresponding one calculated with the HGGA methods. The inclusion of the solvent did not significantly affect the position of the maximum with respect to the gas phase. However, changes in intensity and spectrum-resolution by changing the halide ligand emerged. These observations, which agree with the one experimentally detected,[15] led to B2PLYP in the presence of the solvent to be the best performer in studying UV−vis spectra of the rhenium complexes included in this work.

The assignation of the origin of the band studied showed dependence on the method. While with the HGGA functional a cluster-to-halide-ligand charge transfer (CLCT) may be assumed, B2PLYP consistently leads to an intracluster charge transfer (ICCT) in all cases. This assignment propose by us is in contrast with the experimental results[3,9,15] and with the one made available by Arratia et al.,[10] which considered the origin of the density transfer to be halide ligand-to-metal charge transfer (LCCT). It deserves to be highlighted that the assignment CLCT proposed in this work by us is in line with the experimental explanation of the origin of the band at 416 nm proposed by Shores et al.[20] for the cyanide-bridged cluster $[Re_6Te_8(CN)_6]^{4-}$.

Finally, we strongly recommended the use of the double-hybrid B2PLYP in studying the UV−vis spectrum of rhenium complexes of size making the computational cost affordable.

Acknowledgment. We thank PEDECIBA-QUÍMICA and CSIC for financial support.

Supporting Information Available: Absorption spectra of $[Re_6S_8X_6]^{4-}$ ($X^- = Cl^-$, Br^-, I^-) obtained with HGGA-based methods. This material is available free of charge via the Internet at http://pubs.acs.org.

References and Notes

(1) Kozlova, S. G.; Gabuda, S. P.; Brilev, K. A.; Mironov, Y. V.; Fedorov, V. E. *J. Phys. Chem. A* **2004**, *108*, 10565.

(2) Gray, T. G.; Rudzinski, C. M.; Meyer, E. E.; Nocera, D. G. *J. Phys. Chem. A* **2004**, *108*, 3238.

(3) Gray, T. G.; Rudzinski, C. M.; Meyer, E. E.; Holm, R. H.; Nocera, D. G. *J. Am. Chem. Soc.* **2003**, *125*, 4755.

(4) Deluzet, A.; Duclusaud, H.; Sautet, P.; Borshch, S. A. *Inorg. Chem.* **2002**, *41*, 2537.

(5) Gabriel, J.-C. P.; Boubekeur, K.; Uriel, S.; Batail, P. *Chem. Rev.* **2001**, *101*, 2037.

(6) Yoshimura, T.; Umakoshi, K.; Sasaki, Y.; Ishizaka, S.; Kim, H.-B.; Kitamura, N. *Inorg. Chem.* **2000**, *39*, 1765.

(7) Saito, T. *J. Chem. Soc., Dalton Trans.* **1999**, 97.

(8) Gray, T. G.; Rudzinski, C. M.; Nocera, D. G.; Holm, R. H. *Inorg. Chem.* **1999**, *38*, 5932.

(9) Guilbaud, C.; Deluzet, A.; Domercq, B.; Molinié, P.; Coulon, C.; Boubekeur, K.; Batail, P. *Chem. Commun.* **1999**, 1867.

(10) Arratia-Pérez, R.; Acevedo-Hernández, L. *J. Chem. Phys.* **1999**, *110*, 2529.

(11) Arratia-Pérez, R.; Acevedo-Hernández, L. *J. Chem. Phys.* **1999**, *111*, 168.

(12) Beauvais, L. G.; Shores, M. P.; Long, J. R. *Chem. Mater.* **1998**, *10*, 3783.

(13) Zheng, Z.; Long, J. R.; Holm, R. H. *J. Am. Chem. Soc.* **1997**, *119*, 2163.

(14) Mironov, Y. V.; Cody, J. A.; Albrecht-Schmitt, T.; Ibers, J. A. *J. Am. Chem. Soc.* **1997**, *119*, 493.

(15) Long, J. R.; Mc Carty, L. S.; Holm, R. H. *J. Am. Chem. Soc.* **1996**, *118*, 4603.

(16) Gancheff, J. S.; Denis, P. A.; Hahn, F. E. *J. Mol. Struct. (THEOCHEM)* **2010**, *941*, 1.

(17) Lee, C.; Yang, W.; Parr, R. G. *Phys. Rev. B* **1988**, *37*, 785.

(18) Gancheff, J. S.; Denis, P. A.; Hahn, F. E. *Spectrochim. Acta, Part A* **2010**, *76*, 348.

(19) Gancheff, J. S.; Albuquerque, R. Q.; Martínez-Guerrero, A.; Pape, T.; De Cola, L.; Hahn, F. E. *Eur. J. Inorg. Chem.* **2009**, 4043.

(20) Grimme, S. *J. Chem. Phys.* **2006**, *124*, 34108.

(21) Grimme, S.; Goerigk, L. *J. Phys. Chem. A* **2009**, *113*, 767.

(22) Grimme, S.; Neese, F. *J. Chem. Phys.* **2007**, *127*, 154116.

(23) Perdew, J. P.; Ruzsinszky, A.; Tao, J. M.; Staroverov, V. N.; Scuseria, G. E.; Csonka, G. I. *J. Chem. Phys.* **2005**, *123*, 062201.

(24) Ruzsinszky, A.; Perdew, J. P.; Csonka, G. I. *J. Chem. Theory Comput.* **2010**, *6*, 127.

(25) Constantin, L. A.; Pitarke, J. M.; Dobson, J. F.; Garcia-Lekue, A.; Perdew, J. P. *Phys. Rev. Lett.* **2008**, *100*, 036401.

(26) Dobson, J. F.; Wang, J.; Gould, T. *Phys. Rev. B* **2002**, *66*, 081108.

(27) Biczysko, M.; Panek, P.; Scalmani, G.; Bloino, J.; Barone, V. *J. Chem. Theory Comput.* **2010**, *6*, 2115.

(28) Shores, M. P.; Beauvais, L. G.; Long, J. R. *J. Am. Chem. Soc.* **1999**, *121*, 775.

(29) Becke, A. D. *Phys. Rev. A* **1998**, *38*, 3098.

(30) Tao, J.; Perdew, J. P.; Staroverov, V. N.; Scuseria, G. E. *Phys. Rev. Lett.* **2003**, *91*, 146401.

(31) Becke, A. D. *J. Chem. Phys.* **1993**, *98*, 5648.

(32) Perdew, J. P.; Burke, K.; Ernzerhof, M. *Phys. Rev. Lett.* **1996**, *77*, 3865.

(33) Adamo, C.; Barone, V. *J. Chem. Phys.* **1999**, *110*, 6158.

(34) Becke, A. D. *J. Chem. Phys.* **1993**, *98*, 1372.

(35) Pyykkö, P. *The Effect of Relativity in Atoms, Molecules and The Solid State*; Plenum: New York, 1990.

(36) Barone, V.; Cossi, M. *J. Phys. Chem. A* **1998**, *102*, 1995.

(37) Cossi, M.; Rega, N.; Scalmani, G.; Barone, V. *J. Comput. Chem.* **2003**, *24*, 669.

(38) O'Boyle, N. M.; Tenderholt, A. L.; Langner, K. M. *J. Comput. Chem.* **2008**, *29*, 839.

(39) Frisch, M. J.; Trucks, G. W.; Schlegel, H. B.; Scuseria, G. E.; Robb, M. A.; Cheeseman, J. R.; Scalmani, G.; Barone, V.; Mennucci, B.; Petersson, G. A.; Nakatsuji, H.; Caricato, M.; Li, X.; Hratchian, H. P.; Izmaylov, A. F.; Bloino, J.; Zheng, G.; Sonnenberg, J. L.; Hada, M.; Ehara, M.; Toyota, K.; Fukuda, R.; Hasegawa, J.; Ishida, M.; Nakajima, T.; Honda, Y.; Kitao, O.; Nakai, H.; Vreven, T.; Montgomery, J. A., Jr.; Peralta, J. E.; Ogliaro, F.; Bearpark, M.; Heyd, J. J.; Brothers, E.; Kudin, K. N.; Staroverov, V. N.; Kobayashi, R.; Normand, J.; Raghavachari, K.; Rendell, A.; Burant, J. C.; Iyengar, S. S.; Tomasi, J.; Cossi, M.; Rega, N.; Millam, N. J.; Klene, M.; Knox, J. E.; Cross, J. B.; Bakken, V.; Adamo, C.; Jaramillo, J.; Gomperts, R.; Stratmann, R. E.; Yazyev, O.; Austin, A. J.; Cammi, R.; Pomelli, C.; Ochterski, J. W.; Martin, R. L.; Morokuma, K.; Zakrzewski, V. G.; Voth, G. A.; Salvador, P.; Dannenberg, J. J.; Dapprich, S.; Daniels, A. D.; Farkas, Ö.; Foresman, J. B.; Ortiz, J. V.; Cioslowski, J.; Fox, D. J. *Gaussian 09, Revision A.1*; Gaussian, Inc.: Wallingford, CT, 2009.

JP110100W